Supplementary information's

Oxygen evolution catalytic behaviour of Ni doped Mn_3O_4 in alkaline medium

V. Maruthapandian,* T. Pandiarajan, V. Saraswathy* and S. Muralidharan

CSIR-Central Electrochemical Research Institute, Karaikudi-630003, Tamilnadu, India.

Tel phone: +91-4565-241393, +91-4565-241359; Fax: +91-4565-227779
E-mail: maruthuori.tn@gmail.com and corrsars@gmail.com

1. X-ray diffraction patterns

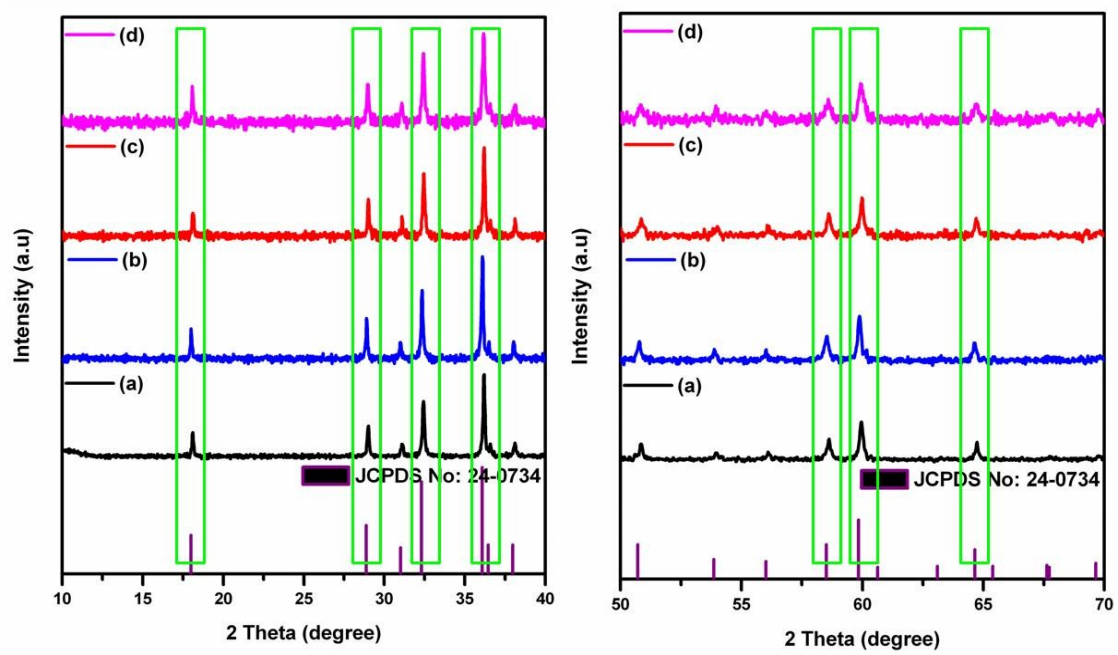

Fig. S1. X-ray diffraction patterns of Mn_3O_4 and Ni doped Mn_3O_4 in which (a) bare Mn_3O_4, (b) 1 wt% Ni doped Mn_3O_4, (c) 5 wt% Ni doped Mn_3O_4 and (d) 10 wt% Ni doped Mn_3O_4.

Spinel (AB_2O_4) based metal oxide are of great interest in the recent years in variety of technological applications due to the mixed valent metal cations of A^{2+} and B^{3+} offers more possible option to replace the metal cations to tune the desirable properties and applications vice versa. In Mn_3O_4, The Mn exists as Mn^{2+} in A site and Mn^{3+} in B site. Based on these principles recently, the catalytic, supercapactive and magnetic properties of Mn_3O_4 are tuned by the doping of Ni, Co and Cr.[1-3] In this regard, the present study is the evaluation of catalytic behavior of Mn_3O_4 by the doping of Ni in the form of Ni^{2+} ion in A lattice of Mn_3O_4. The doping is possible due to the closest ionic radii of Mn^{2+} (0.80 Å) and Ni^{2+} (0.69Å).

While doping of Ni^{2+} in the Mn_3O_4, the tetrahedral site Mn^{2+} ion are partially doped /replaced/substituted by the Ni^{2+} ions, in mean time the octahedral site contains the Mn^{3+} ions as

such without any substitution.[2] Fig. S1 shows the XRD patterns of the present study of bare Mn_3O_4 and 1, 5 and 10 wt% Ni doped Mn_3O_4 samples. In the XRD patterns no characteristics peak changes are observed (the peaks are highlighted in Fig S1). It is due to the previously mentioned same ionic radii of dopant of Ni and comparably very low level of Ni doping (Ni is doped 1, 5 and 10 wt% on the basis of total wt% in the Mn_3O_4). This similar trend in XRD pattern is observed in the recent studies of Cr, Co, Ni and Cu doped Mn_3O_4 and Cr doped $NiFe_2O_4$.[1-4]

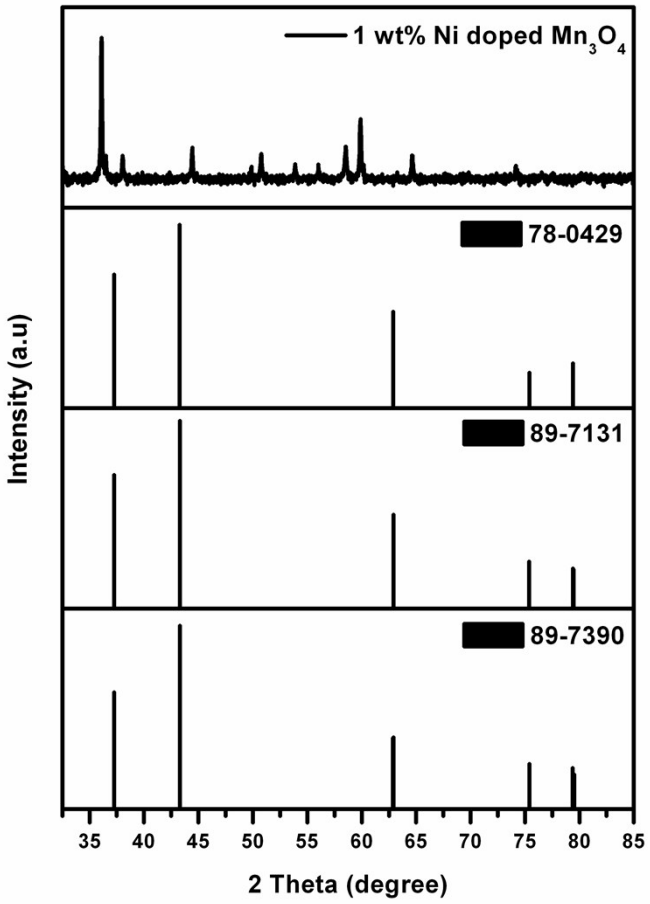

Fig. S2. X-ray diffraction pattern of 1 wt% Ni doped Mn_3O_4 with standard diffraction patterns of NiO

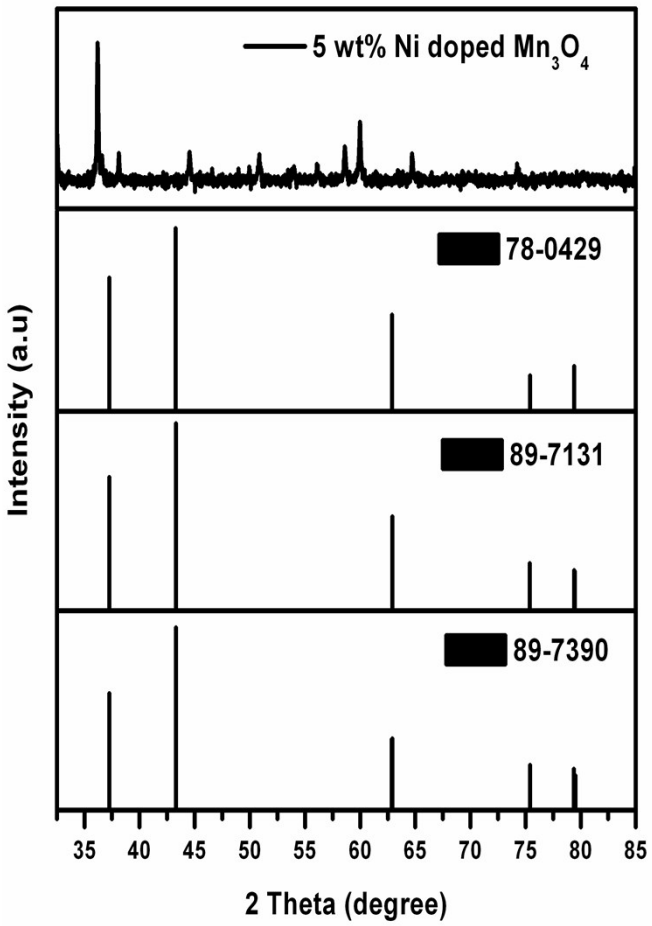

Fig. S3. X-ray diffraction of pattern of 5 wt% Ni doped Mn_3O_4 with standard diffraction patterns of NiO

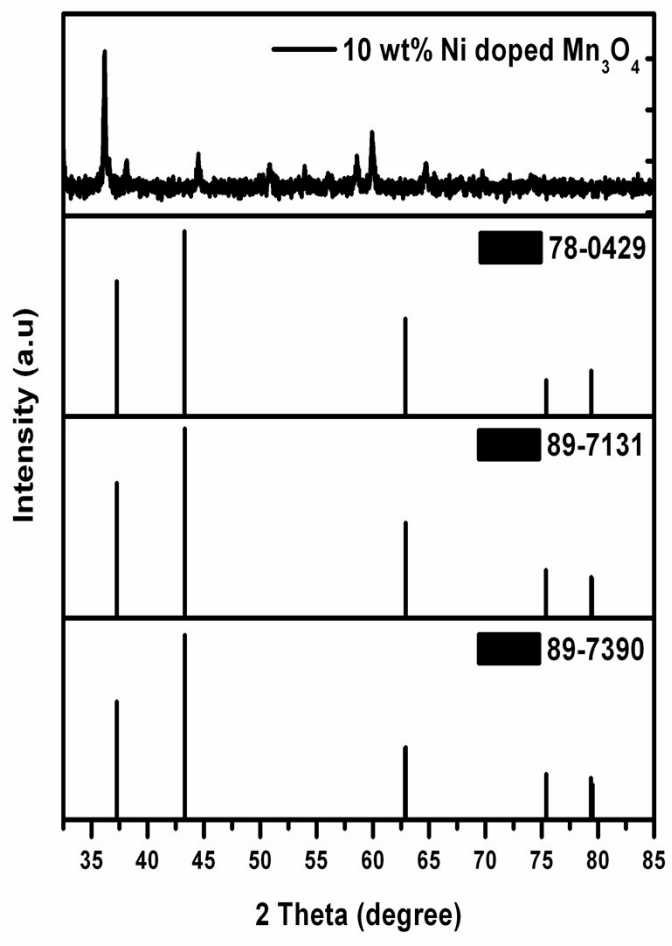

Fig. S4. X-ray diffraction of pattern of 10 wt% Ni doped Mn_3O_4 with standard diffraction patterns of NiO

2. Selected area diffraction studies for lattice parameters

Table S1. Calculated lattice parameter of Mn_3O_4 through the SAED

2R in pix	R in 1/nm	Calculated D space in Å	JCPDS No 24-0734 D space in Å	hkl
161.47	2.0183	4.9544	4.9240	101
261.84	3.2730	3.0553	3.0890	112
322.67	4.0333	2.4793	2.4870	211
326.22	4.0777	2.4523	2.4630	202
344.45	4.3056	2.3225	2.3670	004
447.69	5.5961	1.7869	1.7988	105
511.69	6.3961	1.5634	1.5762	321
521.49	6.5186	1.5340	1.5443	224
613.65	7.6706	1.3036	1.2777	413

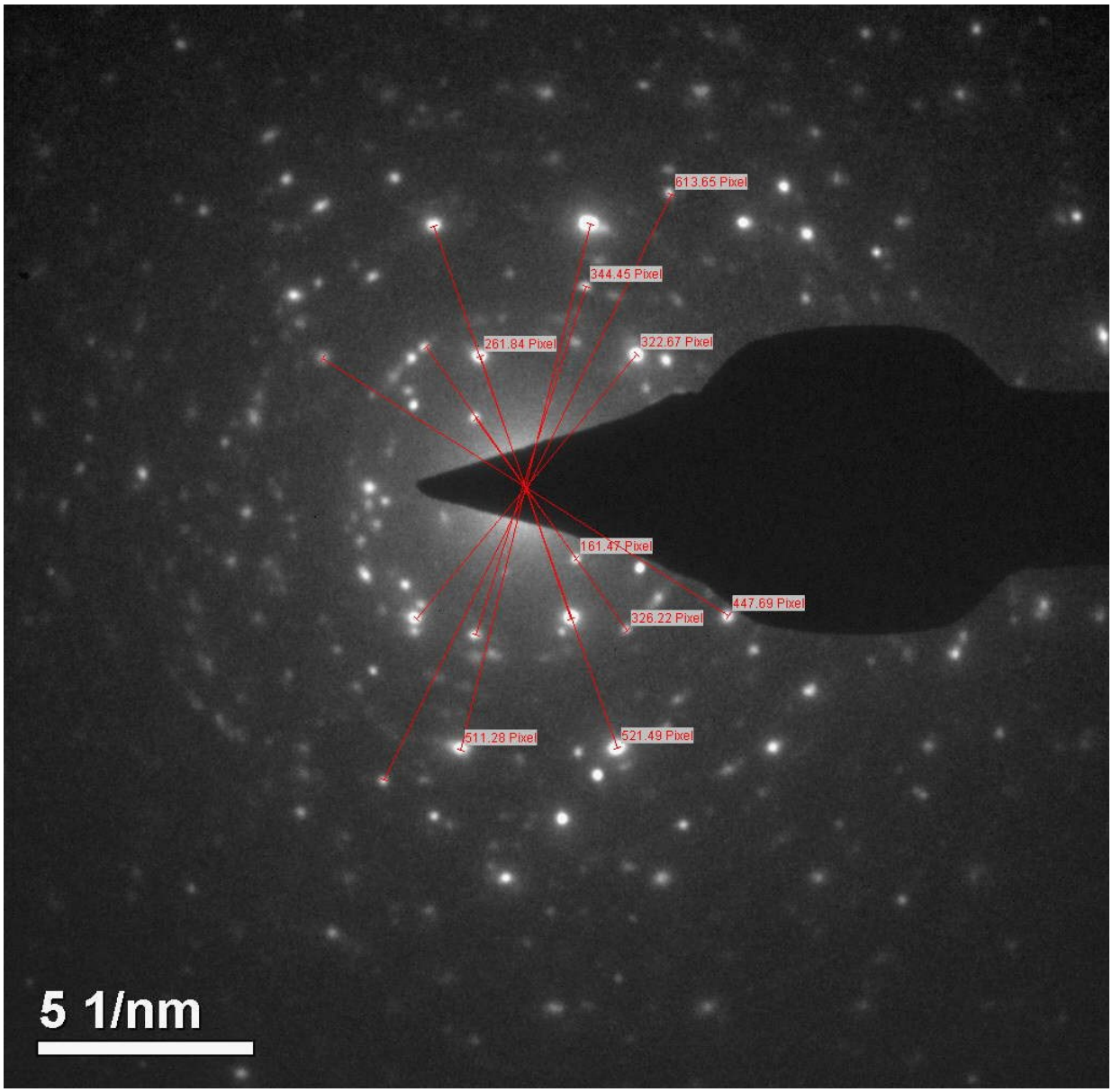

Fig. S5. Selected area diffraction pattern Mn_3O_4 (5 nm = 200 pixel).

Table S2. Calculated lattice parameter of 10 wt% Ni doped Mn_3O_4 through the SAED

2R in pix	R in 1/nm	D space in Å	JCPDS No 24-0734 D space in Å	hkl
409.42	4.0942	2.4424	2.4870	211
509.22	5.0922	1.9637	2.0369	220
589.07	5.8907	1.6975	1.7008	312

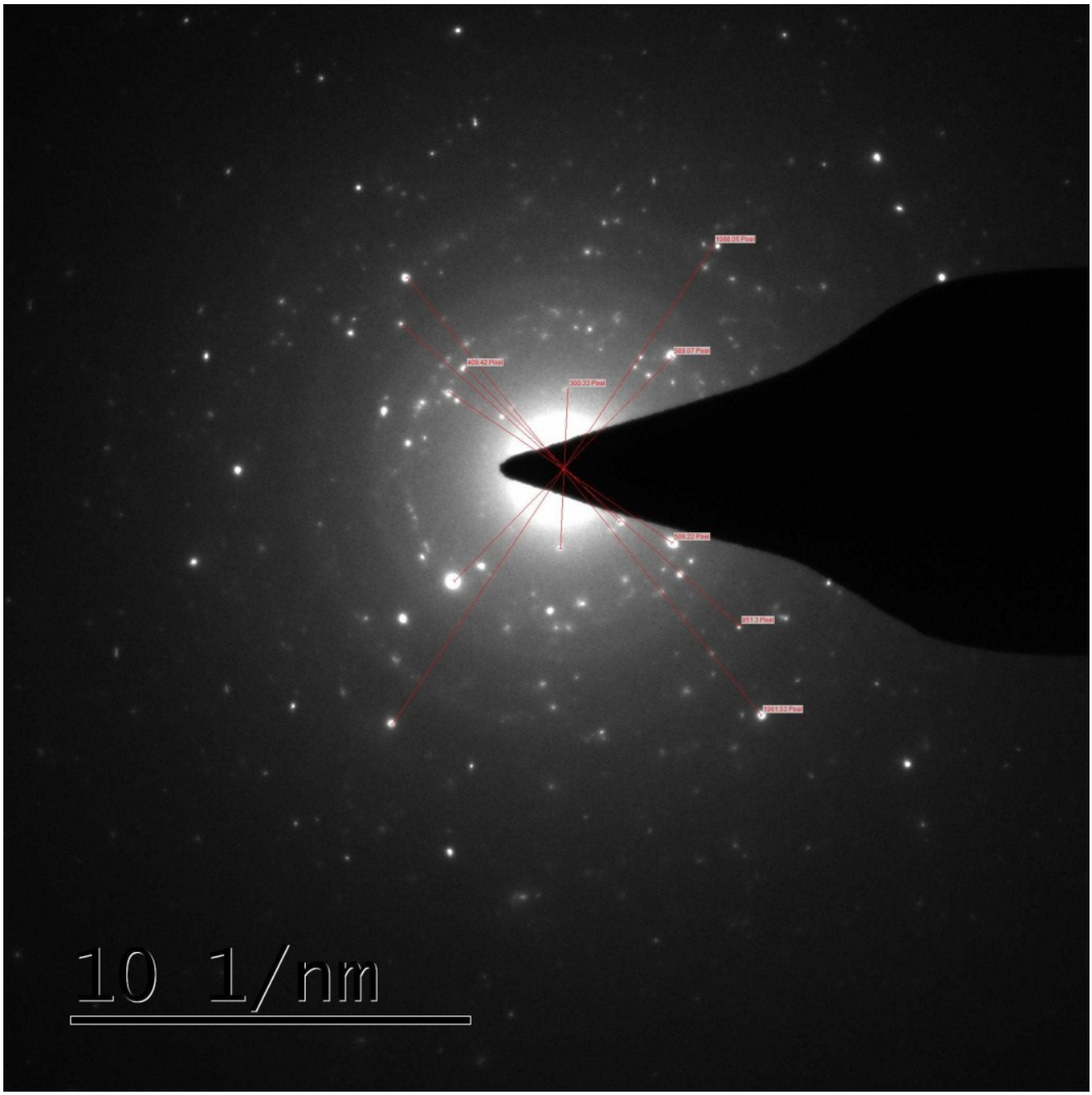

Fig. S6. Selected area diffraction patter of 10 wt% Ni doped Mn_3O_4 (10 nm = 500 pixel).

The measured diameter of SAED in pixel unit is not visible in the Fig. S6 as such condition. It is visible under magnification only.

3. **Elemental mapping of Mn and Ni**

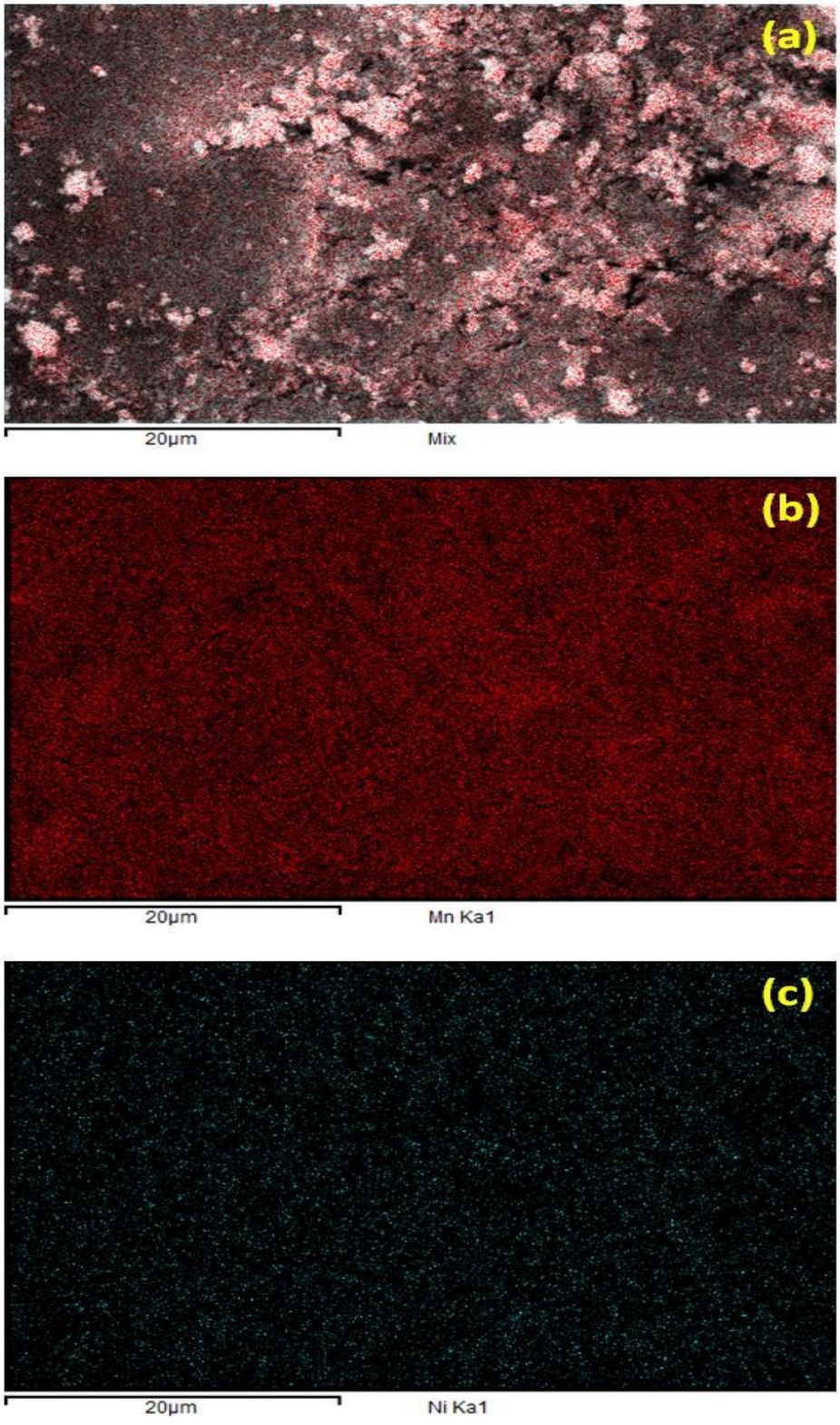

Fig. S7. Elemental mapping of Mn and Ni in 10 wt% Ni doped Mn_3O_4.

Table S3.Elemental compostion of as prepared 10 wt% ni doped Mn_3O_4 by EDS analysis.

Element	Weight %	Atomic %	Compd %	Formula
Mn K	69.23	44.93	89.39	MnO
Ni K	8.34	5.07	10.61	NiO
O	22.43	50.00		
Totals	100.00			

4. Atomic absorption spectrum studies

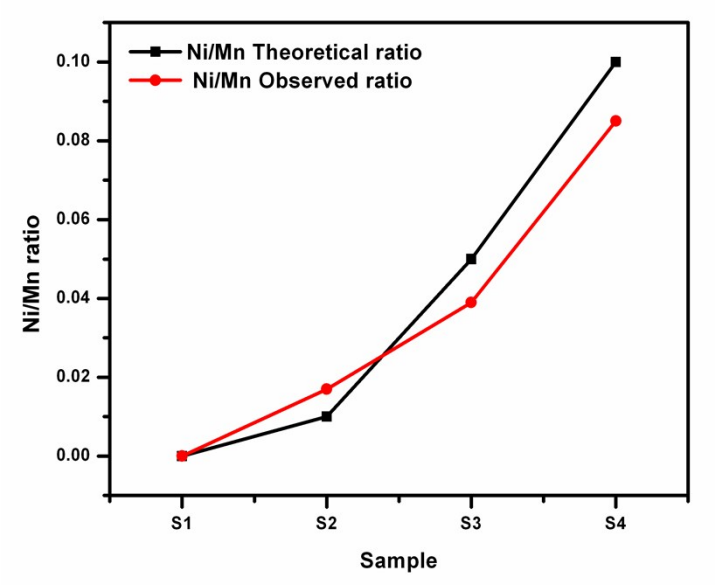

Fig. S8. Theoretical and observed Ni/Mn ratio of Mn_3O_4 and Ni doped Mn_3O_4. Where S1) Mn_3O_4, S2) 1 wt% Ni doped Mn_3O_4, S3) 5 wt% Ni doped Mn_3O_4 and S4) 10 wt Ni doped Mn_3O_4.

5. FTIR spectrum studies

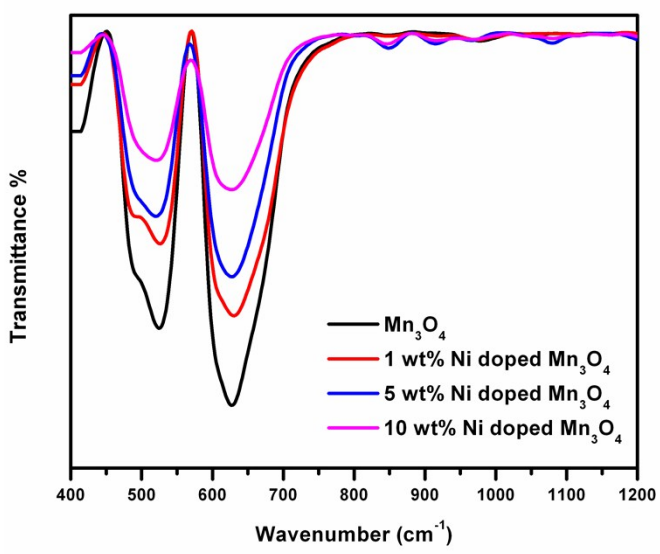

Fig. S9. FTIR spectrum of Mn_3O_4 and Ni doped Mn_3O_4.

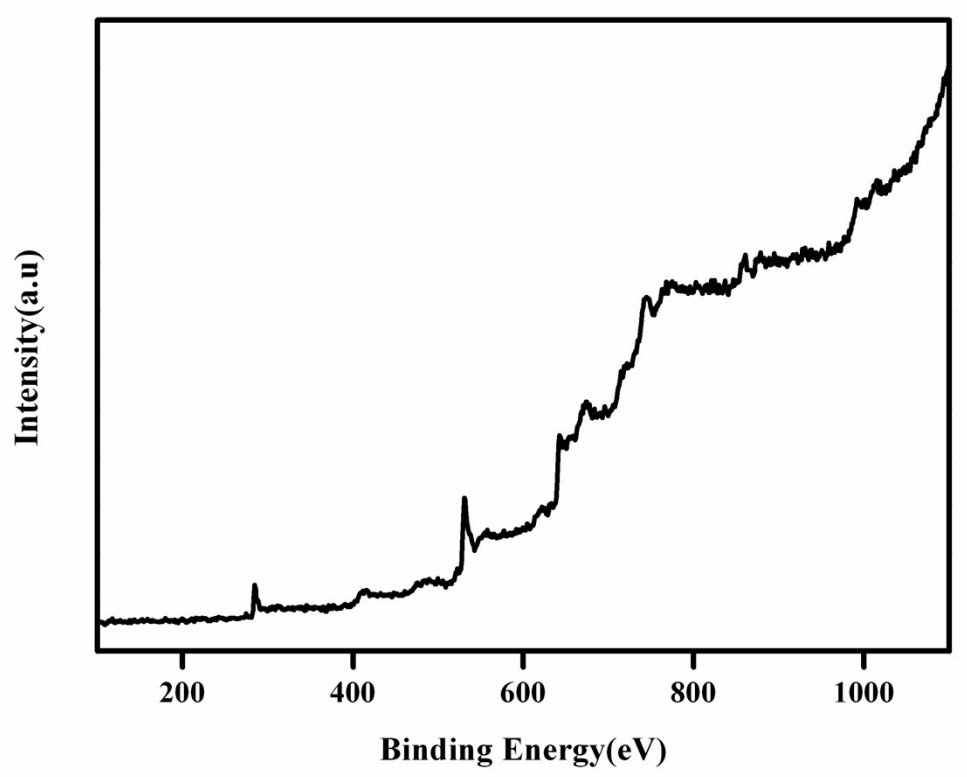

Fig. S10. Survey spectrum of 10 wt% Ni doped Mn_3O_4.

6. Micro-structural characterizations

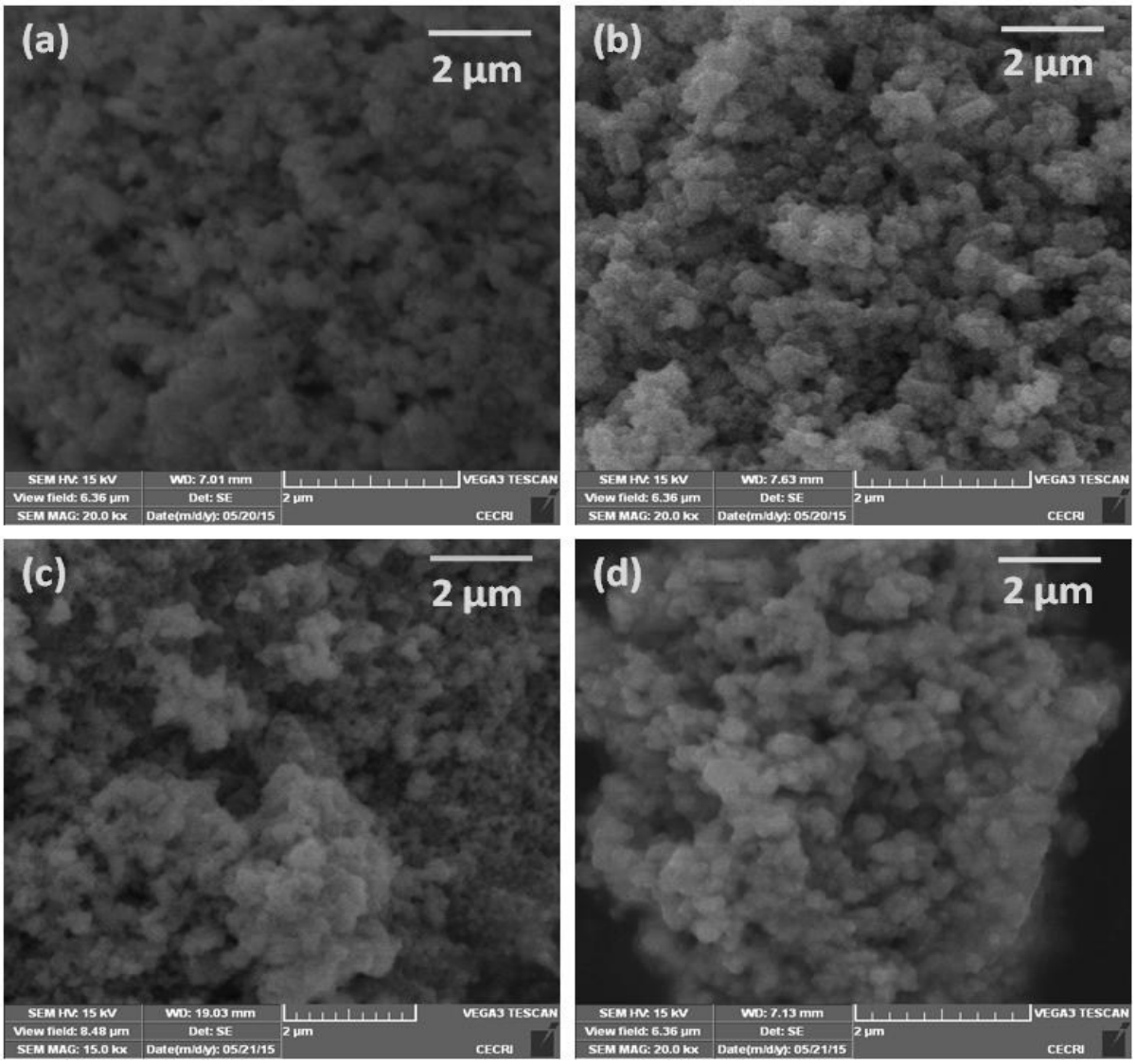

Fig. S11. SEM images of a) Mn_3O_4, b) 1 wt% Ni doped Mn_3O_4, c) 5 wt% Ni doped Mn_3O_4 and d) 10 wt % Ni doped Mn_3O_4.

7. Cyclic stability of 10 wt% Ni doped Mn_3O_4

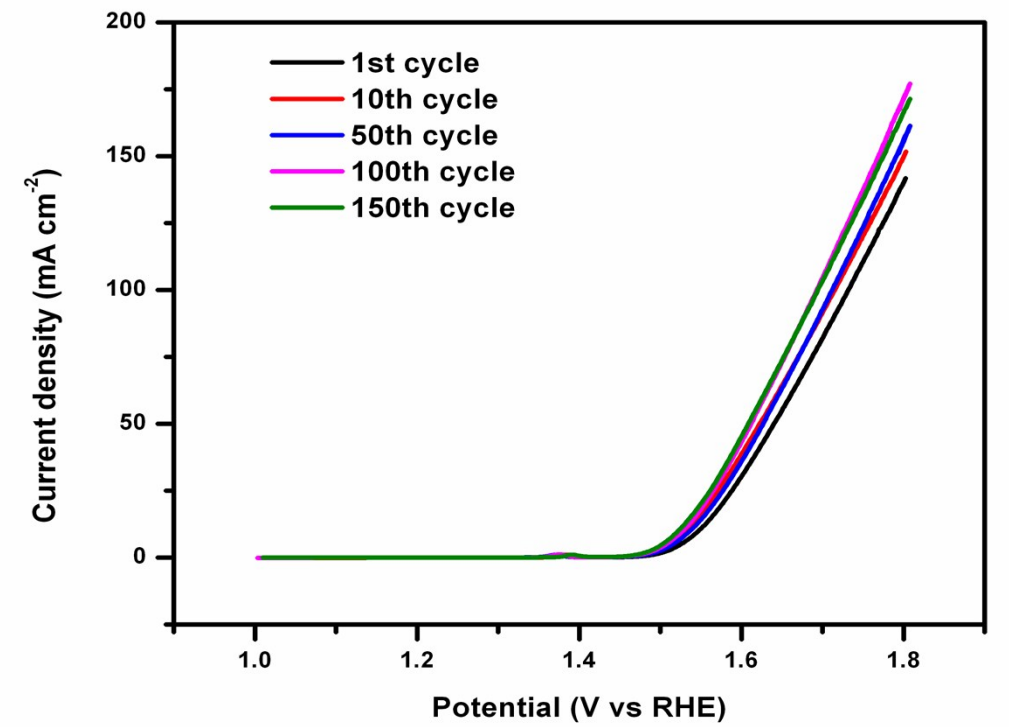

Fig. S12. Catalytic cyclic stability of 10 wt% Ni doped Mn_3O_4 from the cyclic voltammetry data anodic part recoded at the scan rate of 2 mV s^{-1} in 1 M KOH.

References

1. G. Li, X. B. Tang, S. Y. Lou, and S. M. Zhou, *Appl. Phys. Lett*., 2014, **104**, 173105.
2. S. Hirai, S. Yagi, A. Seno, M. Fujioka, T. Ohno and T. Matsuda, *RSC Adv*., 2016, **6**, 2019.
3. R. Dong, Q. Ye, L. Kuang, X. Lu, Y. Zhang, X. Zhang, G. Tan, Y. Wen and F. Wang, *ACS Appl. Mater. Interfaces*., 2013, **5**, 9508.
4. R.N. Singh, J.P. Singh, B. Lala, M.J.K. Thomasb, S. Bera, *Electrochimica Acta*., 2006, **51** 5515.